Fine Structure and Dynamics of the Solar Atmosphere
Proceedings IAU Symposium No. 327, 2016
S. Vargas Domínguez, A.G. Kosovichev, P. Antolin & L. Harra, eds.

doi:10.1017/S1743921317004008

Evidence of in-situ Type II radio bursts in interplanetary shocks

S. M. Díaz-Castillo[1], J. C. Martínez Oliveros[2] and B. Calvo-Mozo[1]

[1]Observatorio Astronómico Nacional, Universidad Nacional de Colombia
Bogotá, Colombia
email: smdiazcas@unal.edu.co, bcalvom@unal.edu.co

[2]Space Sciences Laboratory, University of California, Berkeley, USA
email: oliveros@ssl.berkeley.edu

Abstract. We present a database of 11 interplanetary shocks associated to coronal mass ejections (CMEs) observed by STEREO and Wind missions between 2006 and 2011 that show evidence of Type II radio burst. For all events, we calculated the principal characteristics of the shock driver, the intensity and geometrical configuration of the in-situ shock and checked for the existence of in-situ type II radio burst. We made a comparative analysis of two CME events (on 18 August 2010 and 4 June 2011), which are apparently associated to two or more magnetic structures which interact in space (i.e. CMEs, SIRs, CIRs). These events show varied shock configurations and intensities. We found evidence of in-situ type II radio bursts in one of the events studied, suggesting that the geometry of the shock (quasi-perpendicularity) is also critical for the generation and/or detection of radio emission in-situ.

Keywords. coronal mass ejections (CMEs), shock waves, solar radio emission

1. Introduction

Interplanetary shocks are generated by the speed differences between upstream propagating structures and the interplanetary medium, and are often associated with Interplanetary Coronal Mass Ejections (ICMEs), Stream Interaction Regions (SIRs) or Corotating Interaction Regions (CIRs) (Sheeley *et al.*1985, Schwenn *et al.*1986, Cane *et al.*1986). It is generally accepted that shock waves accelerate particles leading to the generation of radio waves, plasma waves and under certain physical conditions may trigger geomagnetic phenomena (Howard 2011). In-situ observations of interplanetary shock are characterized by abrupt changes of the plasma parameters, such as speed, density, pressure, magnetic field and temperature, and in the interplanetary medium case are classified as fast or slow shocks or as forward or reverse shocks (Lepping 2005).

It is generally accepted that type II bursts are caused by shock waves in the corona and CME-driven shocks in the solar wind (Cane *et al.*1987 Reiner *et al.*1998). Shock accelerated electrons excite Langmuir waves, which, through non-linear wave-wave interactions, drive coherent radio emission at the local electron plasma frequency f_{pe} or its harmonics (e.g. $2f_{pe}$) (Ginzburg & Zhelezniakov 1958). This radio emission has a functional dependency of the local plasma density, $f_{kHz} \sim \sqrt{n_e}(cm^3)$. Hence, as the electron density decreases with radial distance, so the frequency of the radio burst, which can be seen in the dynamic radio spectra as a frequency drift in time (Wild & McCready 1950; Wild *et al.*1954; Nelson & Melrose 1985; Gopalswamy 2004). Type II radio bursts are generally associated with propagating CMEs and other structures such as CIRs, including their interaction, which can produce shock waves (e.g. Burlaga *et al.*1987, Gopalswamy *et al.*2001, Reiner *et al.*2003, Cho *et al.*2007, 2008, 2011, Martínez-Oliveros *et al.*2012, Martínez-Oliveros *et al.*2015)

When a propagating interplanetary shock reaches a spacecraft, clear changes of the plasma parameters can be detected. Bale *et al.*1999 described an interplanetary foreshock region and the associated in-situ type II radio emission, suggesting the existence of an inhomogeneous large-scale structure of CME-driven shock front. They suggest a magnetic connection to a quasi-perpendicular shock front acceleration site based on the observation of Langmuir waves. Prior to these observations, type II bursts were considered as a diffuse background emission with sporadic intensification and it was suggested that some sporadic type II emissions correspond to emission at multiple and distinct sites along the shock front (Cane *et al.*1987; Reiner *et al.*1998). However, it is still an open question where on the CME-driven shock surface the type II burst is generated. (e.g., Cliver *et al.*1999, Oh *et al.*2007, Vršnak, & Cliver 2008, Magdalenić *et al.*2008, Liu *et al.*2009)

In the following sections we show the data sample selection criteria, along with the basic features of the radio emission and associated in-situ shock, and finally a comparative analysis of two events of the sample as case studies.

2. Selected events: Data sample

We constructed a database of CME and flares associated to in-situ shocks and radio emissions. From this sample, we selected 11 CME-driven shock events observed by the STEREO and Wind missions between 2006 and 2011. During this period the spatial configuration of the spacecrafts covers a wide angular range and their separation give us insight of the spatial characteristics of the propagating shocks. We then evaluate the CME morphology and kinematics using remote observations (Coronal and heliospheric observations made by coronographs and radio burst dynamic spectra). Table 1 shows the summary of the basic analysis of the selected events, which includes the characteristics of the progenitors, as well as the characteristics of the radio emission and the detected shock in-situ.

At least two of the selected events are linked to X-class GOES flares, and 64% of the CMEs propagate with speeds larger than 900 km/h. All events are related to type II radio burst but only 45% show emission at frequencies lower than 500 kHz. The observations suggest that the events are related to fast forward type shocks, however the energetic and geometric characteristics are varied. 45% of the shocks have quasi-perpendicular configuration ($\theta_{B_n} > 60°$). Only 35% have a Mach Alfvén number (M_A) greater than 4 surpassing the maximum value predicted by the Rankine-Hugoniot conditions (Cairns 2011). We found evidence of in-situ Type II radio burst and possibly Langmuir waves for two cases, for which the shock is characterized as quasi-perpendicular (See last column on Table 1).

As case studies, we will describe the events of 18 August 2010 and 4 June 2011. Those events are selected due to its wide and continuous frequency range in the type II radio emission (See Table 1 Type II radio burst initial and final detection), in such way that the best remote tracking of the shock front can be made, making its characterization more accurate. We determine the optimal physical configurations of the shocks, the characteristic of the radio emission and describe the apparent interaction between different transient events such as CMEs, CIRs or streamers with the radio burst generation or observation.

3. CME-SIR interaction of 18 August 2010

On 18 August 2010 a CME was observed by the STEREO A, SOHO and Wind. The flare associated with this CME produced an intense type III radio burst and the initial detection of the type II radio burst was at high frequencies. This type II radio burst

https://doi.org/10.1017/S1743921317004008 Published online by Cambridge University Press

Table 1. Database of selected events. Most of the events present evidence of Flares, Type II radio burst and interplanetary shock. Only 2 events of the sample present evidence of Type II radio burst in-situ

Event Time		Flare	CME		Type II radio burst [1]		In-situ interplanetary shock[2]					In-situ Type II burst (Langmuir Waves)
Inital(Release)	Final(Shock)	Goes class	SPC[3]	V_{Proj} (km/s)[4]	Initial (kHz)	Final (kHz)	SPC[3]	Shock type	θ_{Bn} [5]	V_{Shock} (km/s)	M_A [6]	
2006/12/13 2:40	2006/12/14 13:51	X3.4	SOHO	1700	12000	150	Wind	FF[7]	33±63	919±465	6.8±2.6	-
2007/05/19 12:57	2007/05/22 1:59	B9.5	SOHO - STB - STA	900	15000	13000	STA	FF	41±7	520±29	1.1±0.3	-
2008/04/26 13:54	2008/04/29 14:10	B3.8	SOHO - STB	650	-	-	STB	FF	69±9	432±12	1.9±0.1	-
2008/05/17 10:16	2008/05/19 16:39	B1.7	SOHO - STB	600	10000	1200	STB	FF	29±11	640±49	2.3±0.6	-
2010/03/01 22:58	2010/03/04 3:51	B6.5	SOHO - STB	1200	3000	300	STB	FF	34±34	415±392	0.3±0.3	-
2010/08/01 9:10	2010/08/03 17:05	-	STB - STA	-	2000	700	Wind	FF	70±12	531±34	4.8±0.7	2010/08/03 17:05
2010/08/07 18:24	2010/08/11 9:31	M1.0	STB - STA	900	13000	700	STB	FF	76±52	297±41	2.0±1.0	-
2010/08/18 5:48	2010/08/20 16:13	C4.5	SOHO - STA	1500	12000	20	STA	FF	65±3	553±11	2.5±0.1	2010/08/20 16:13
2011/02/15 2:10	2011/02/18 0:49	X2.2	SOHO - STB - STA	750	16000	400	Wind	FF	80±13	424±40	5.5±0.7	-
2011/05/09 20:51	2011/05/12 4:45	C5.4	SOHO - STB	1200	16000	900	STB	FF	5±17	544±176	4.7±3.0	-
2011/06/04 21:45	2011/06/05 18:59	-	SOHO - STA	2000	16000	25	STA	FF	45±44	636±163	2.5±1.1	-

Notes:
[1] We compare our results with the Wind/WAVES type II bursts and CMEs database from CDAW Data Center (`http://cdaw.gsfc.nasa.gov/`)
[2] The shock parameters were calculated using the method described in the Heliospheric Shock Database of the University of Helsinki (`http://ipshocks.fi/`)
[3] Spacecraft
[4] Coronograph projected speed
[5] Angle between velocity flux and the ambient magnetic field direction
[6] Upstream mach number
[7] Fast Forward shock

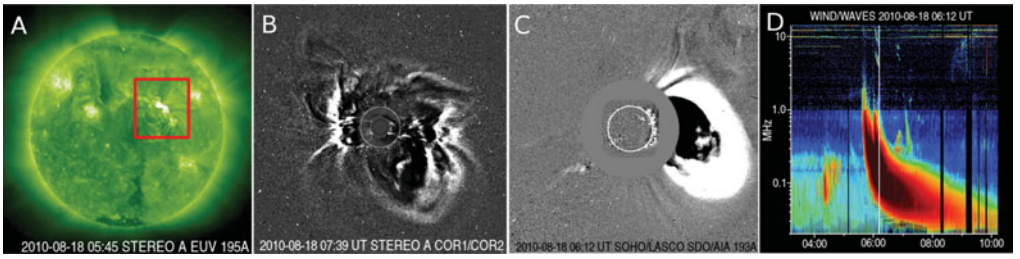

Figure 1. *A*: STEREO A EUV chromospheric image at 195 Å showing the hosting active region. *B*: STEREO A COR1/COR2, *C* SOHO/LASCO coronagraph images showing the first stages of CME propagation. *D*: Wind/WAVES dynamic radio spectra showing the Type III and II radio burst.

we believe is associated with a long duration and slow-drifting feature in the dynamic radio spectra observed. We noticed that 13 hours after the onset of the CME, in-situ fast forward interplanetary shock, along with Langmuir waves were detected. Figure 1 shows the location of the hosting active region AR 11099 (A), STEREO and LASCO observations of the CME (B,C) and the radio burst at the beginning of the event (D).

By analyzing the j-maps and in-situ data between 17:00UT on August 20 to 00:00UT on August 21, we notice what seems to be a streamer, which we believe had some direct association with the generation of the slow drift type II emission, hence, indicating the propagation of a slow shock. The shock reached STEREO-A on 21 August at 16:13 UT, as seen by the in-situ and radio instruments on Wind. Figure 2 shows the plasma observation of the foreshock upstream region of the shock, where electrons are reflected and forming a beam distribution which later triggers Langmuir waves. Based on the temporal analysis of the j-maps and dynamic radio spectra we observe a possible interaction of a streamer with the CME , suggesting the formation of a fast forward shock and therefore the slow drift radio emission (Cairns 2011) (See red boxes on figure 2).

https://doi.org/10.1017/S1743921317004008 Published online by Cambridge University Press

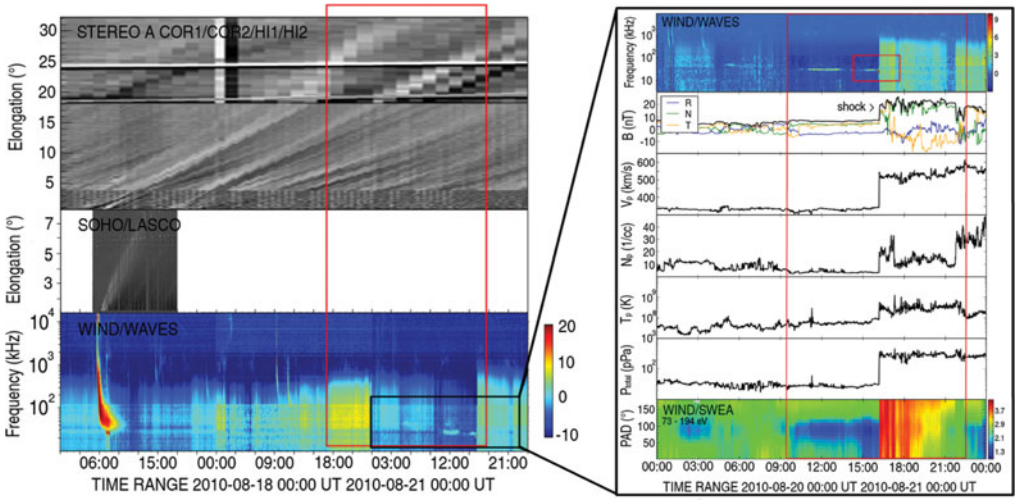

Figure 2. *Left*: STEREO A COR1/COR2/HI1/HI2 and SOHO/LASCO j-maps and dynamic radio spectra for August 18, 19 and 20 showing the temporal evolution of the CME. *Right*: STEREO A PLASTIC/IMPACT/SWEA particle in-situ data showing in-situ interplanetary shock features at 16:13UT on August 20.

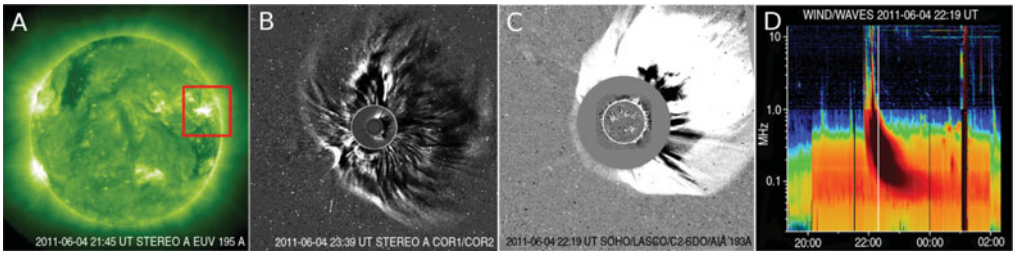

Figure 3. *A*: STEREO A EUV chromospheric image at 195 Åshowing the hosting active region. *B:* STEREO A COR1/COR2 and *C:* SOHO/LASCO coronagraph images showing the first stages of the CME at 21:45UT on June 4.*D* Wind/WAVES dynamic radio spectra showing the Type III and II radio burst.

4. CME-CME interaction of 4 June 2011

This event is associated to apparently a CME-CME interaction of June 4, 2011 observed by STEREO A, SOHO and Wind. Two CMEs were generated by the same active region AR 11222 at 7:00UT and 21:45UT on 4 June 2011. Figure 3 shows the hosting active region (A), LASCO imagery of the studied CME (B, C) and the radio burst at the beginning of the event (D). An intense type III radio burst was associated to both transients.

Figure 4 shows the j-maps and radio dynamic spectra of the event. The type II radio bursts were clearly observed from the onset of both events. In particular, between 9:00UT and 13:00UT on 5 June a broad and intense type II radio emission is detected. An in-situ fast forward interplanetary shock without evidence of an in-situ type II radio burst was observed 36 hours later of the first CME release(See figure 4). In addition to the shock, in this event it is possible to clearly differentiate the frontal region of compression yielded by the CME bulk structure. Finally, it is also possible to distinguish the characteristics of two independent magnetic clouds (See figure 4).

https://doi.org/10.1017/S1743921317004008 Published online by Cambridge University Press

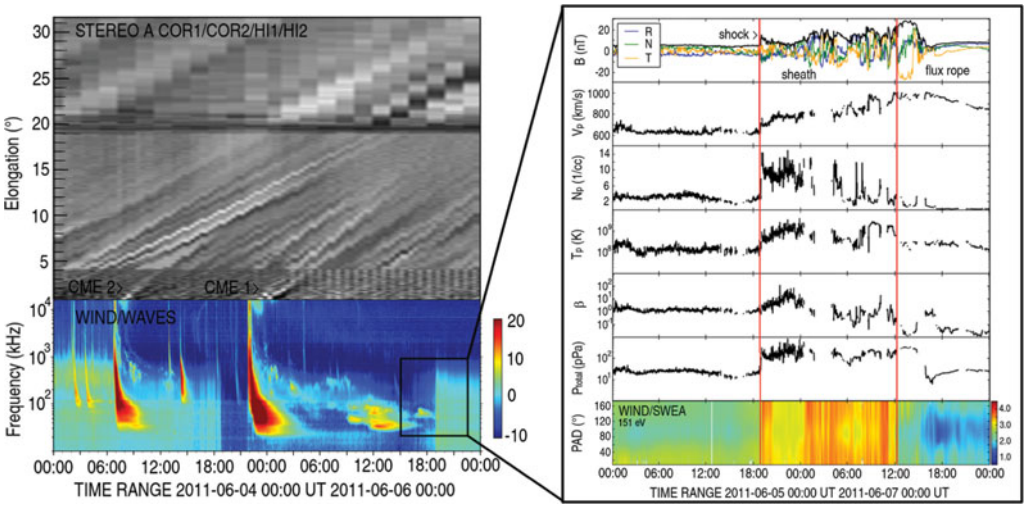

Figure 4. *Left*: STEREO A COR1/COR2/HI1/HI2 j-maps and dynamic radio spectra for June 4 and 5 showing the temporal evolution for both CMEs. *Right*: STEREO A PLASTIC/IMPACT/SWEA particle data showing in-situ interplanetary shock features at 18:59 UT on June 5.

5. Discussion

In this article we described the selection criteria used to build a database for the study of radio emissions related to interplanetary shocks. From this database two events of 18 August 2010 and 4 June 2011 were selected and a description of the main features and their analysis was made.

In our first study case (18 August 2010), coronagraph and heliospheric imagery along with the dynamic radio spectra suggest the interaction between a CME and a streamer. This complex interaction triggered the formation of a fast forward shock in a quasi-perpendicular configuration (See Table 1) which produced the radio emission. For this event the structure of flux rope or magnetic cloud after the shock is not clearly observed.

The CMEs in our second case study (4 June 2011) had a propagation speeds of ≈2000 km/s, which easily produced CME-driven shocks associated directly to the type II radio emission. In this case we do not observe direct evidence of in-situ radio emission or Langumir waves. The observed radio emission is a slow drifting event lasting a couple of days. This suggests that the apparent interaction between both CMEs is producing a continuous propagating magnetosonic shock modulated in intensity by the solar wind conditions around it. However, we do not rule out the possibility that the radio emission can also modeled by CME-SIR or CME-CIR interactions.

We also propose a simple scenario of propagation for both events as shown in figure 5. In this scenario we assume a cone geometry and propagated the structure along the projected direction as seen from the coronagraph images. The angular dimension of the propagated structure is the reported CME angular width. Although this simple scenario is usually used to describe the morphological structure of CMEs (two-dimensional and simple geometric forms) and is highly inaccurate for reproducing complex scenarios, it is useful to obtain an initial general understanding of CME associated events, e.g. the CME front of the event of 18 August passes through STA, which ensure us that the shock and radio emission in situ corresponds to the studied CME-driven shock.

https://doi.org/10.1017/S1743921317004008 Published online by Cambridge University Press

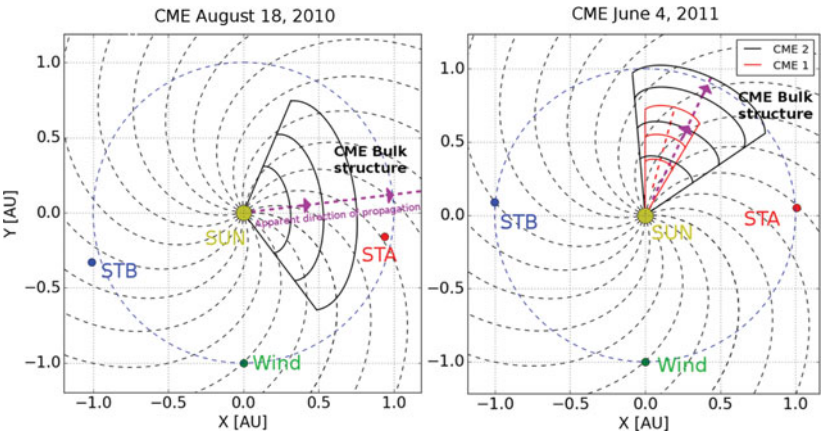

Figure 5. Cone model for CMEs of both events in the interplanetary medium. *Left*: CME 18 August. *Right*: CME 4 June 1: 21:45UT CME 2: 7:00UT.

References

Bale, S. D., Reiner, M. J., Bougeret, J. L., *et al.* 1999, *Geophys. Res. Lett.*, 26, 1573

Burlaga, L. F., Behannon, K. W., & Klein, L. W. 1987, *J. Geophys. Res.*, 92, 5725

Cairns, I. H. 2011, *The Sun, the Solar Wind and the Heliosphere, ed. M. P. Millares & J. Sánchez* (IAGA Special Sopron Book Series Vol.4 Springer), 267

Cane, H. V., Kahler, S. W., & Sheeley, N. R., Jr. 1986, *J. Geophys. Res.*, 91, 13321

Cane, H. V., Sheeley, N. R., Jr., & Howard, R. A. 1987, *J. Geophys. Res.*, 92, 9869

Cliver, E. W., Webb, D. F., & Howard, R. A. 1999, *Sol. Phys.*, 187, 89

Cho, K. S., Lee, J., Moon, Y. J., *et al.* 2007, *A&A*, 461, 1121

Cho, K. S., Bong, S. C., Kim, Y. H., *et al.* 2008, *A&A*, 491, 873

Cho, K. S., Bong, S. C., Moon, Y. J., *et al.* 2011, *A&A*, 530, 16

Filbert, P. C. & Kellogg, P. J. 1979, *J. Geophys. Res.*, 84, 1369

Ginzburg V. L. & Zhelezniakov V. V. 1958, *SvA*, 2, 653

Gopalswamy, N., Yashiro, S., Kaiser, M. L., *et al.* 2001, *Astrophys. J.*, 548, 1L91

Gopalswamy, N. 2004, *Planet. Space Sci.*, 52, 1399

Howard, T. 2011, *Coronal Mass Ejections: An Introduction*, (Springer),p. 17

Lepping, R. P. 2005, *Solar wind shock waves and discontinuities*, (IOP Publishing),p. 1

Liu, Y., Luhmann, J. G., Bale, S. D., & Lin, R. P. 2009, *ApJ*, 691, L151

Magdalenić, J., Vršnak, B., Pohjolainen, S., *et al.* 2008, *Sol. Phys.*, 253, 305

Martínez Oliveros, J. C., Raftery, C. L., Bain, H. M., *et al.* 2012, *Astrophys. J.*, 748, 1L6

Martínez Oliveros, J. C., Raftery, C., Bain, H., Liu, Y., *et al.* 2015, *Sol. Phys.*, 290, 3891

Nelson, G. J. & Melrose, D. B. 1985, *In Solar Radiophysics: Studies of Emission from the Sun at Metre Wavelengths, ed. D. J. McLean & N. R. Labrum* (Cambridge: Cambridge Univ. Press), 333

Oh, S. Y., Yi, Y., & Kim, Y. H. 2007, *Sol. Phys.*, 245, 391

Pulupa, M. & Bale, S. D. 2008, *ApJ*, 676 2, 1330

Reiner, M. J., Kaiser, M. L., Fainberg, J., & Stone, R. G. 1998, *J. Geophys. Res.*, 103A12, 29651

Reiner, M. J., Vourlidas, A., Cyr, O. C. St., *et al.* 2003, *ApJ*, 590, 533

Sheeley, N. R., Jr., Howard, R. A., Michels, D. J., *et al.* 1985, *J. Geophys. Res.*, 90, 163

Schwenn, R. 1985, *Space Sci. Rev.*, 44, 139

Terasawa, T. 2011, *The Sun, the Solar Wind and the Heliosphere, ed. M. P. Millares & J. Sánchez* (IAGA Special Sopron Book Series Vol.4 Springer), 121

Vršnak, B. & Cliver, E. W. 2008, *Sol. Phys.*, 253, 215

Wild, J. P., Murray, J. D., & Rowe, W. C. 1954, *Aust. J. Sci. Res. A*, 7, 439

Wild, J. P. & McCready, L. L. 1950, *Aust. J. Sci. Res. A*, 3, 387

https://doi.org/10.1017/S1743921317004008 Published online by Cambridge University Press